Journal of Animal Environment

(E-ISSN 2717-1396, ISSN 2717-1388)

Assessment of Microplastic Susceptibility Zones in the Gadilam River Basin, Tamil Nadu, India, Using a GIS-Based Analytic Hierarchy Process

***E. Nivetha[1]and Dr.R. Mathiyazhagan[2]**

1. Research Scholar, Annamalai University
2. Professor, department of Civil engineering, Annamalai University

Corresponding author: nivethae96@gmail.com

ABSTRACT

Microplastic occurrence in river basins is heterogeneous; however, South Asia basin-scale assessments have relied on point-based sampling, limiting coverage. This study delineates microplastic susceptibility zones across the Gadilam River Basin (1,396.76 km²) in Tamil Nadu by integrating twelve source, pathway, and terrain parameters such as runoff, land use/land cover (LULC), population density, the normalized difference built-up index (NDBI), slope, drainage density, flow accumulation, and distances to dump sites, industries, markets, waterbodies and hospitals within a GIS-based AHP. The Pairwise comparison assigned the largest weights to runoff (17.61%), distance to dump sites (14.29%), LULC (14.02%) and population density (14.01%). Weighted linear combination produced a susceptibility index ranging from 176.47 to 482.17 were classified into five zones: Very Low (19.64%), Low (35.60%), Moderate (30.39%), High (8.84%) and Very High (5.54% of basin area). Among the 342 revenue villages within the basin, 27 villages, accounting for 7.89%, were classified as High, while 20 villages, representing 5.85%, were categorized as Very High. These villages are predominantly located in the central and lower regions of the basin, where waste sources, developed land, and monsoon-driven runoff converge over areas of low-gradient terrain. Kruskal–Wallis tests with false-discovery-rate correction showed that eleven of the twelve factors differed significantly among classes, and epsilon-squared effect sizes ranked distance to dump sites ($\varepsilon^2 = 0.39$), population density (0.36), runoff (0.26) and LULC (0.26) as the strongest discriminators, converging independently with the AHP weighting. The 47 High and Very High villages constitute a bounded priority set for field-based microplastic monitoring, dump-site remediation and urban runoff management.

Keywords: microplastics; susceptibility zonation; analytic hierarchy process; GIS; multi-criteria decision-making; Gadilam River Basin

INTRODUCTION:

Microplastics are plastic particles smaller than 5 mm. They were first recognized as a unique type of environmental pollutant in the early 2000s and have been found in marine, freshwater, and land environments (Thompson et al., 2004). Global plastic production and poor waste management have led to large amounts of plastic waste entering the environment. Early global estimates suggest that land-based sources contribute several million tonnes to the ocean each year (Jambeck et al., 2015). Once released, microplastics break down slowly compared to most organic pollutants. Their small size and low density enable them to travel long distances through water, wind, and living organisms (Mitrano et al., 2021). This combination of persistence, mobility, and widespread occurrence has led to microplastics being increasingly recognised as a contaminant of concern in environmental management, even as the ecological and human health consequences of chronic exposure continue to be characterised rather than fully established. In this broader context, freshwater systems, especially river basins, play a critical role. Rivers act as primary channels linking terrestrial sources of plastic waste to downstream lakes, estuaries, and coastal waters. A substantial portion of the plastic debris entering the ocean is thought to originate from transport facilitated by rivers (Lebreton et al., 2017). Microplastics produced on land are moved, spread, and either temporarily or permanently retained within a catchment through hydrological processes such as surface runoff, channel flow, and sediment transport (Range et al., 2023). Microplastics enter river systems from a range of urban, industrial, domestic, and waste-management-related sources, including treated and untreated wastewater discharge (Kay et al., 2018). Microplastic distribution within a river basin is seldom consistent due to the significant variation in inputs and the hydrological routes that transport them across a catchment. Studies compiling data from multiple sites have demonstrated that microplastic concentrations can differ by several orders of magnitude, even in similar environments (Yu et al., 2025). Microplastic pollution within a river basin constitutes not merely a localized water-quality issue but also a spatially distributed phenomenon at the watershed scale. This is influenced by both the origin of contaminants and the efficiency with which the basin transports them. A critical review of the anthropogenic and environmental factors relevant to this study clarifies that not all spatial variables relate to microplastic occurrence in the same way. Population density and the extent of urban and built-up land use have been

***Corresponding Author:**
Received: 25th May, 2026; Revised: 6th July, 2026; Accepted: 28th July, 2026; Available Online: 29th August, 2026
(DOI): 10.70102/AEJ.2026.18.8s.19

repeatedly associated with elevated microplastic abundance in river water and sediment, reflecting the concentration of domestic, commercial, and traffic-related plastic use in densely settled areas (Ta and Babel, 2023). The Normalized Difference Built-up Index, derived from short-wave and near-infrared reflectance, provides a remote-sensing-based surrogate for the intensity and extent of such built-up land cover and is therefore a useful proxy for urbanisation-related pressure (Zha et al., 2003). Industrial regions, municipal dumpsites, and wastewater treatment plants represent more direct point and diffuse sources especially landfill leachate has been shown to transport microplastics into surrounding soil and groundwater including in studies conducted in South Indian dumpsite settings (Manikanda Bharath et al., 2021), while treated effluent from wastewater treatment plants consistently increases microplastic loading in receiving rivers even after conventional treatment (Kay et al., 2018; Zhang et al., 2025). Healthcare facilities have similarly been identified as a source of microplastic-bearing effluent by virtue of their reliance on single-use plastic materials (Kamani et al., 2024). In contrast, slope, drainage density, flow accumulation, runoff, and proximity to streams are better understood as transport and connectivity variables: they do not generate microplastics but influence how readily particles mobilised from source areas are conveyed into the channel network and distributed downstream. Land use and land cover occupies an intermediate position, since it captures both source intensity, through built-up and industrial land, and surface characteristics that influence runoff generation. This distinction between source-related, transport-related, and land cover variables that mediate both roles is important, since it clarifies that the twelve criteria considered in this study are not treated as equally or directly causal but as indicators contributing differently to relative susceptibility. Conventional field-based monitoring, while essential for establishing actual microplastic concentrations, faces recognised practical limitations when the objective is to characterise an entire river basin. Sampling and laboratory analysis of microplastics remain labour-intensive, and existing basin-scale datasets show pronounced spatial and temporal heterogeneity that complicates comparison across studies with differing sampling density and methodology (Yu et al., 2025). Many case studies have also been found to under-represent spatiotemporal variability, and the transport pathways linking sources to eventual sinks within a catchment remain incompletely characterised even where monitoring has occurred (Range et al., 2023). Given the cost and logistical demands of establishing a monitoring network with sufficient spatial density to characterise an entire basin, there is a clear rationale for approaches that can screen and prioritise areas of relatively higher susceptibility ahead of, or in support of, targeted field sampling. Such an approach does not substitute for direct measurement of microplastic concentration; rather, it provides a relative spatial indication of where source pressure and transport potential jointly suggest a greater likelihood of microplastic occurrence or accumulation, and is best understood as a screening and prioritisation tool.

Geographic Information System-based multi-criteria Decision-Making offers a suitable framework for this purpose because it allows heterogeneous spatial datasets, spanning hydrological, land-use, and anthropogenic pressure indicators, to be standardised and integrated into a single composite index. Among available MCDM techniques, the Analytic Hierarchy Process, which structures a decision problem hierarchically and derives criterion weights through pairwise comparison, has become one of the most widely applied methods in environmental susceptibility and vulnerability mapping, including for landslide, flood, and groundwater vulnerability assessment (Saaty, 1980; Bansal et al., 2023; Zewdie et al., 2024). A recent application of GIS-based AHP to riverscape pollution vulnerability along the Ganga demonstrated the method's capacity to integrate population density, land use, slope, drainage density, and rainfall into a single vulnerability surface, while also illustrating the sensitivity of AHP outputs to the underlying expert-derived weighting scheme (Acciavatti et al., 2024). This last point is worth stating explicitly: AHP is a decision-support and weighting framework grounded in expert judgement and literature-supported relative importance rather than a mechanistic model of microplastic generation or transport, and its outputs should accordingly be interpreted as an index of relative susceptibility rather than a validated prediction of contaminant flux. Despite the growing application of GIS-based AHP to flood, landslide, and groundwater vulnerability assessment, its use in the specific context of microplastic pollution remains limited. Existing basin- and national-scale microplastic assessments have generally relied on point-based field sampling combined with pollution or ecological risk indices calculated at discrete stations, an approach that, while valuable for characterising measured concentrations, does not provide continuous spatial coverage across a catchment and can be sensitive to differences in sampling density between studies (Yu et al., 2025). Conversely, GIS-AHP applications to river pollution vulnerability have so far addressed general water-quality or wastewater-related pressure rather than microplastic-specific source, transport, and accumulation dynamics (Acciavatti et al., 2024). A basin-scale framework that integrates a broad set of source variables, including dumpsites, wastewater treatment plants, hospitals, industrial regions, and built-up intensity, together with hydrological

connectivity variables such as drainage density, flow accumulation, runoff, slope, and stream proximity, specifically for the purpose of delineating microplastic susceptibility zones, has not been established for river basins in South Asia. This gap forms the basis for the present study. The Gadilam Basin, located in Tamil Nadu, southern India, provides a relevant setting in which to address this gap. The basin encompasses both hard-rock and sedimentary aquifer systems and has been the subject of several hydrogeochemical investigations that document the presence of industrial activity, including lignite mining operations and associated industrial complexes, within and adjacent to the catchment (Aravindan et al., 2004; Prasanna et al., 2010). The lower part of the basin lies within Cuddalore district, which hosts a designated industrial estate whose effluent management has been the subject of monitoring by state pollution control authorities (Central Pollution Control Board, 2018). The basin drains toward the Bay of Bengal, so that land-based pressures generated upstream have the potential to be conveyed toward the coast through the drainage network. Taken together with the documented industrial and hydrogeological characteristics of the basin, these features suggest that the Gadilam Basin combines several of the source and transport conditions relevant to microplastic susceptibility, while, to the extent existing literature indicates, having not previously been assessed for this purpose using a spatial multi-criteria approach.

This study integrates twelve criteria: slope, runoff, drainage density, flow accumulation, distance to dumpsites, streams, industrial regions, wastewater treatment plants, and hospitals, population density, land use/land cover, and the Normalized Difference Built-up Index, within a GIS-based AHP-MCDM framework to delineate microplastic susceptibility zones across the Gadilam Basin. By combining source-related, transport-related, and land-cover-mediated indicators into a single composite susceptibility index, the resulting spatial output is intended to support the identification of priority areas for future field-based microplastic monitoring, inform pollution-source management, and provide a decision-support framework that can assist watershed-level environmental planning and the prioritisation of mitigation interventions in the basin.

2. MATERIALS AND METHODS

2.1 Study Area

The Gadilam River Basin is a east-flowing coastal watershed in the northern part of Tamil Nadu, south-eastern India, lying between approximately 11°38′ and 11°56′ N latitude and 79°00′ and 79°46′ E longitude, and draining an area of approximately 1,397 km² before discharging into the Bay of Bengal near Cuddalore (Fig. 1). The basin spans parts of the Kallakuruchi, Viluppuram and Cuddalore districts and lies within the humid tropical belt of the Coromandel Coast. The Gadilam rises in the low uplands to the west and follows a broadly west-to-east course across gently sloping terrain, so that most of the basin is characterised by low relief. Slope analysis confirms this configuration: more than two-thirds of the basin has gradients below six degrees, and only a narrow upland fringe exceeds this value. The drainage network is dendritic and moderately developed, with drainage density ranging from near zero in the flatter reaches to about 9.9 km/km² in the more dissected uplands.

The regional climate is tropical wet and dry, and rainfall is dominated by the north-east monsoon between October and December. Mean annual rainfall across the Gadilam basin, as expressed through the runoff surface derived in this study, varies spatially between roughly 370 and 540 mm, and the concentration of rainfall within a short monsoon window generates strong seasonal surface flow. Land use is mixed and reflects intense human occupation of a coastal lowland. Built-up land and fallow land each account for approximately one-third of the basin, cropland occupies close to one-fifth, and the remaining area is distributed among plantation, barren land and surface water. The lower and central parts of the basin include the urban and peri-urban expansion around Cuddalore together with associated industrial establishments, market centres, hospitals and informal waste-disposal sites. This combination of a densely occupied low-gradient coastal plain, a monsoon-driven flow regime and a short transport distance to the sea makes the basin a relevant setting in which to evaluate the terrestrial pressures that govern microplastic susceptibility.

The assessment follows a source to pathway to susceptibility to spatial-prioritisation logic. Terrestrial microplastics are generated at anthropogenic sources such as waste-disposal sites, densely populated and built-up areas, market clusters and industrial establishments. Once released, particles are mobilised and redistributed by hydrological and terrain-controlled pathways, including surface runoff, the drainage network and low-gradient accumulation zones, before reaching potential receiving environments such as the river channel and connected waterbodies (Xia et al., 2025; Gao et al., 2024). Twelve anthropogenic and hydrological variables that represent these source and pathway components were integrated within a geographic information system using the analytic hierarchy process (AHP) to produce a composite microplastic susceptibility index. The output expresses the relative propensity of each location to receive and retain terrestrial microplastics. It is important to state that the model estimates relative susceptibility and does not measure microplastic concentration, because no field concentration data were collected. The framework therefore identifies

where source pressure and transport potential coincide, in a manner consistent with geospatial risk-factor overlays applied to microplastics elsewhere (Australian biosolid-application hotspot mapping; Beheshtimaal et al., 2024).

2.2 Data sources and preprocessing

Twelve thematic layers were compiled from openly available remote-sensing products, national datasets and visually digitised features (Table 1). Terrain variables were derived from the 30 m Shuttle Radar Topography Mission (SRTM) digital elevation model distributed by the United States Geological Survey (USGS). Land cover and the built-up index were obtained from a cloud-free Landsat 9 OLI-2 scene acquired on 3 March 2026 through USGS Earth Explorer. Rainfall used in runoff estimation was obtained from the India Meteorological Department (IMD), and population density was taken from the WorldPop 1 km UN-adjusted product for 2020. Industrial and hospital layers were obtained from the Tamil Nadu Geographic Information System (TNGIS), while dump-site and market locations were digitised as point features through visual interpretation of high-resolution imagery in Google Earth Pro. All raster layers were projected to a common Universal Transverse Mercator coordinate system, resampled to a uniform 30 m grid and clipped to the basin boundary. Processing was carried out in ArcGIS and QGIS, and statistical plotting was performed in a Python environment.

The proximity layers included in the final model are distance to dump sites, distance to industries, distance to markets, distance to waterbodies and distance to hospitals. Distance to waterbodies was computed from surface-water features rather than from an abstract stream buffer, and distance to markets was compiled from digitised market points. These five proximity criteria, together with runoff, land use and land cover (LULC), population density, the normalised difference built-up index (NDBI), flow accumulation, drainage density and slope, constitute the twelve criteria carried through to weighting, zonation and the village-level analysis.

2.3 Factors Influencing the Microplastic Susceptibility

Each of the twelve criteria was selected because it represents either a source of terrestrial microplastics or a control on their mobilisation, transport and retention, and no factor was included merely to enlarge the model. The criteria fall into three conceptual groups. Source-pressure variables, comprising LULC, population density, NDBI, and distance to dump sites, industries, markets and hospitals, index the intensity and spatial proximity of the human activities that generate plastic waste. Pathway variables, comprising runoff, drainage density and flow accumulation, describe the hydrological mechanisms that detach particles and route them toward the drainage network. The terrain variable, slope, governs flow energy and therefore the balance between through-transport and deposition. For each factor, the direction of its influence on susceptibility is stated explicitly below, because this direction governs how the layer was reclassified onto the common 1–5 scale in Section 2.5. For the five proximity criteria the relationship is inverse, so that a location close to a source or to a receiving feature is more susceptible even though its measured distance is smaller, and it is the reclassified rating rather than the raw distance that carries this meaning forward.

Runoff: Runoff depth was estimated with the Soil Conservation Service curve number (SCS-CN) method, combining IMD rainfall with curve numbers derived from land cover, soil and terrain (Fig. 2). Runoff was retained as the most heavily weighted criterion because surface flow is the principal non-point pathway that detaches terrestrial plastic residues from land surfaces and delivers them to drainage lines. Rainfall first incorporates a large fraction of surface particles into the soil matrix and then exports the remainder in overland flow, so that particle export scales with the volume and intensity of runoff generated during a storm (Ross et al., 2023; Cho et al., 2023). Microplastic concentrations in receiving waters rise measurably following rain events and increase with catchment runoff production and impervious wash-off (Han et al., 2022; Beheshtimaal et al., 2024). This mechanism is especially relevant to the Gadilam Basin, where rainfall is compressed into a short north-east monsoon window that produces intense, episodic surface flow across a low-gradient plain. Higher runoff classes were therefore assigned higher susceptibility ratings.

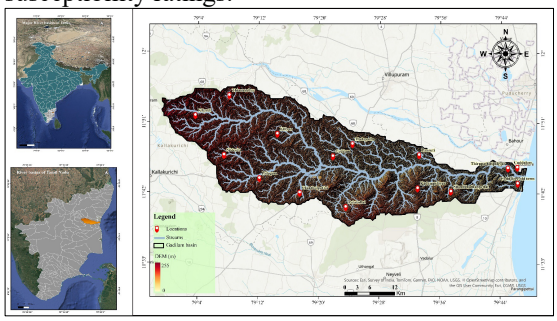


Figure 1. Location and physiography of the Gadilam River Basin, Tamil Nadu, India, showing basin boundary, drainage network and elevation.

Table 1. Datasets, sources, spatial resolution and processing methods for the twelve microplastic susceptibility factors.

Factor	Source	Year	Resolution	Unit	Processing

		/ **date**			
Run off	IMD rainfall and SRTM-derived curve number	2020	30 m	mm yr^{-1}	SCS-CN method in raster calculator
LULC	Landsat 9 OLI-2, USGS	Mar 2026	30 m	classes	Random-forest supervised classification
Population density	WorldPop UN-adjusted	2020	100 m	persons km^{-2}	Rescaled and resampled to basin
Distance to dump sites	Google Earth Pro (digitised)	2026	30m	m	Euclidean distance
Distance to industries	TNGIS	-	30 m	m	Euclidean distance
NDBI	Landsat 9 OLI-2, USGS	Mar 2026	30 m	dimensionless	(SWIR1−NIR)/(SWIR1+NIR)
Flow accumulation	SRTM DEM, USGS	-	30 m	cell count	Flow direction and accumulation
Drainage density	SRTM-derived stream network	-	30 m	km km^{-2}	Line-density computation
Distance to markets	Google Earth Pro (digitized)	2026	30 m	m	Euclidean distance
Distance to waterbodies	Surface-water features (LULC/DEM)	2026	30 m	m	Euclidean distance
Distance to hospitals	TNGIS	-	30 m	m	Euclidean distance

Slope	SRTM DEM, USGS	-	30 m	degrees	Slope tool (terrain analysis)

Land use and land cover: LULC was produced by random-forest supervised classification of the Landsat 9 scene into six classes, namely waterbodies, built-up land, barren land, plantation, fallow land and cropland (Fig. 3). Land cover was included because it integrates, in a single categorical layer, the anthropogenic activity that generates and accumulates plastic waste. Built-up and otherwise disturbed surfaces are repeatedly associated with elevated microplastic loading in catchment and river studies, since they concentrate consumption, waste handling and impervious wash-off, whereas vegetated and water-dominated classes contribute far less to the terrestrial source term (Ranjan et al., 2023; Katusiime et al., 2023). The strength of the land-use signal nevertheless varies with regional context, and some catchments show weaker or inconsistent land-use correlations, so the layer was treated as an indicator of relative source intensity rather than as a deterministic predictor (Talbot and Chang, 2022). Built-up land received the highest rating; cropland, fallow land and barren land received intermediate ratings reflecting mixed anthropogenic disturbance; and plantation and water classes received the lowest ratings.

Population density: Population density, obtained from the WorldPop UN-adjusted product, was used as a direct proxy for the intensity of domestic plastic consumption and disposal (Fig. 4). Densely populated cells generate a proportionally larger per-capita waste stream and, where collection and treatment are inadequate, a larger residual load available for mobilisation, which is why population concentration is consistently linked to higher microplastic abundance in urban and peri-urban river reaches (Ranjan et al., 2023). The layer complements LULC and NDBI by capturing the human occupancy of a given surface rather than its physical cover alone. Higher density classes were rated as more susceptible.

Distance to dump sites: Open and informal dump sites are among the most concentrated terrestrial sources of microplastics, because degrading plastic waste releases fragments and fibres directly to the surrounding soil and to leachate (Fig. 5). Particle concentrations are highest at and immediately around such sites and decline with distance, and open dumping and burning can raise soil microplastic concentrations to levels that rival or exceed those from other diffuse terrestrial sources (Hess et al., 2025; Chamanee et al., 2024). Leachate from these sites acts as a persistent secondary source that migrates to adjacent soil, groundwater and surface water (Kabir et al., 2023; Sun et al., 2024; Lodh et al., 2025). Distance to dump sites was therefore rated inversely, with the nearest cells assigned a rating of five and the most distant cells a rating of one.

Distance to industries: Industrial establishments contribute fibres, fragments and pellets to nearby land and water, and textile and petrochemical operations are recognised point sources in developing-country river systems where effluent treatment is often incomplete (Magalhães et al., 2024; Rahmani et al., 2024). Proximity to industrial areas was included to represent this localised, activity-specific source (Fig. 6), and it was rated inversely so that cells nearer to industry were assigned higher susceptibility.

Normalised difference built-up index: NDBI was computed from the Landsat 9 OLI-2 short-wave infrared and near-infrared bands as NDBI = (SWIR1 − NIR)/(SWIR1 + NIR), corresponding to (Band 6 − Band 5)/(Band 6 + Band 5) (Fig. 7). The index was retained because it provides a continuous, sub-class measure of impervious and built surface that refines the categorical LULC layer and distinguishes densely sealed cores from sparsely built margins within the same built-up class. Impervious surfaces intercept atmospherically and surface-deposited particles and promote their rapid accumulation and wash-off during storms, which links high NDBI values to elevated microplastic delivery (Beheshtimaal et al., 2024). Higher NDBI values were rated as more susceptible.

Flow accumulation: Flow accumulation, derived from flow direction on the DEM, counts the cells draining to each location and therefore identifies convergence zones where water-borne particles are routed and can accumulate (Fig. 8). Cells with high accumulation were rated as more susceptible because they represent potential transport and retention foci within the network. The variable is intrinsically right-skewed, since only the small proportion of cells that coincide with channels attains high values, and this property constrained its discriminatory power at the 30 m resolution used.

Drainage density: Drainage density expresses the length of stream channel per unit area and indexes how efficiently a location is connected to the drainage network (Fig. 9). Denser networks shorten the travel path between source areas and the main channel and accelerate the delivery of mobilised particles, and hydrological connectivity exerts a strong control on riverine microplastic transport and retention (Xia et al., 2025). Higher drainage density was therefore rated as more susceptible.

Distance to markets: Market and commercial clusters are localised generators of single-use

plastic, packaging and film, and commercial land uses record some of the highest microplastic concentrations among urban land-use types in stormwater and sediment surveys (Yuan et al., 2023). Distance to markets (Fig. 10) was rated inversely, so that cells closer to market centres were assigned higher susceptibility.

Distance to waterbodies: Distance to surface waterbodies represents the length of the terrestrial pathway that a mobilised particle must traverse before reaching a receiving or retention environment (Fig. 12). Microplastic concentrations in receiving waters increase with proximity to inputs and outfalls, and short land-to-water distances imply efficient delivery with limited opportunity for interception (Ross et al., 2023; Xia et al., 2025). Cells nearest to waterbodies were therefore rated as most susceptible.

Distance to hospitals: Hospitals consume large volumes of single-use plastic for hygiene and clinical reasons, and a substantial share of healthcare waste is plastic that enters municipal waste and leachate streams, which are themselves established microplastic sources (Kabir et al., 2023; Sun et al., 2024). Distance to hospitals (Fig. 11) was included as an additional localised source proxy and rated inversely. Because direct field evidence linking hospital proximity to riverine microplastics remains limited, this criterion was assigned a low weight and interpreted as a minor, supporting source indicator rather than a primary driver.

Slope: Slope controls flow velocity, sediment transport competence and the tendency toward deposition (Fig. 13). Gentle gradients dissipate flow energy and favour the settling and retention of particles, whereas steep slopes promote rapid through-transport and limited local accumulation, and terrain attributes have been shown to govern the redistribution and retention of microplastics across landscapes (Leitão et al., 2024). Consistent with a retention-oriented interpretation, low-slope cells, which dominate the Gadilam plain, were rated as more susceptible and steep upland cells as least susceptible.

2.4 GIS processing and standardization

All layers were projected to a common UTM grid, resampled to 30 m and clipped to the basin. Each continuous factor was then reclassified into five ordinal susceptibility ratings from 1 (lowest) to 5 (highest) so that heterogeneous variables measured in different units could be combined on a common scale (Table 2). Continuous variables such as runoff, NDBI, flow accumulation, drainage density and slope were binned using natural breaks, and categorical LULC classes were assigned ratings according to their expected source strength. The direction of each rating was set on the basis of the physical rationale given in Section 2.4. For the five distance-based criteria the relationship between proximity and susceptibility is inverse, so that cells nearest to a source or receiving feature received a rating of 5 and the most distant cells received a rating of 1. This distinction is important because the underlying distance values increase away from a feature, whereas the assigned susceptibility rating decreases. The reclassified ratings, not the raw distances, entered the weighted combination.

2.5 Analytic hierarchy process

Relative importance among the twelve criteria was quantified with the AHP (Saaty, 1980, 2008). Pairwise judgements were expressed on Saaty's fundamental 1–9 scale and assembled into a positive reciprocal matrix A, in which element a_{ij} records the importance of criterion i relative to criterion j and a_{ji} equals its reciprocal. The matrix was normalised by dividing each element by its column sum, and the criterion weight w_i was obtained as the mean of each normalised row, which approximates the principal eigenvector of A. The resulting weights are reported in Table 2.

Judgemental consistency was evaluated from the principal eigenvalue λ_{max}, obtained as the mean of the ratio between the weighted sum vector and the corresponding weight for each criterion. The consistency index and consistency ratio were computed as:

$$CI = (\lambda_{max} - n) / (n - 1)$$
$$CR = CI / RI$$

where n is the number of criteria and RI is the random consistency index for a matrix of that order. For the twelve-criterion matrix the analysis yielded λ_{max} = 12.85, giving CI = 0.077. With RI = 1.48 for n = 12, the consistency ratio was CR = 0.052. Because CR is below the conventional 0.10 threshold, the pairwise judgements are internally consistent and the derived weights are acceptable for use in the weighted overlay. The reported ratio was retained as the actual result of the elicited matrix and the judgements were not adjusted to obtain a lower value.

Table 2. Reclassification of the twelve factors into 1–5 susceptibility ratings, class areas, and AHP weights.

S. No.	Parameter	Subclass / Range	Rating	Area (Sq. km)	Area (%)	AHP Weights
1	Runoff (mm/yr)	370.00 – 409.33	1	103.4529	7.41	17.61
		409.33 – 438.00	2	301.6259	21.60	
		438.00 –	3	371.8544	26.62	

		458.00				
		458.00 – 494.67	4	487.8987	34.93	
		494.67 – 540.00	5	131.9298	9.45	
2	**LULC**	Water	1	37.5798	2.69	**14.02**
		Built-up	5	477.161	34.16	
		Barren land	3	16.249	1.16	
		Plantation	2	147.1693	10.54	
		Fallow land	3	472.8653	33.86	
		Cropland	3	245.755	17.60	
3	**Population Density (persons/km²)**	178.20 – 622.93	1	983.3608	70.41	**14.01**
		622.93 – 1290.03	2	299.4634	21.44	
		1290.03 – 2592.45	3	70.8041	5.07	
		2592.45 – 4530.20	4	30.8002	2.21	
		4530.20 – 8278.64	5	12.336	0.88	
4	**Distance to Dump Sites(m)**	5.41 – 4267.52	5	180.4109	12.92	**14.29**
		4267.52 – 7746.80	4	237.3239	16.99	
		7746.80 – 11313.05	3	365.2393	26.15	
		11313.05 – 15227.24	2	351.9456	25.20	
		15227.24 – 22185.79	1	261.3921	18.71	
5	**Distance to Industries (m)**	5.41 – 7528.20	5	141.8955	10.16	**9.04**
		7528.20 – 13770.51	4	193.7697	13.87	
		13770.51 – 20493.00	3	288.3769	20.65	
		20493.00 – 28335.91	2	420.6627	30.12	
		28335.91 – 40820.54	1	352.997	25.27	
6	**NDBI**	−0.32 – −0.14	1	121.7051	8.71	**8.62**
		−0.14 – −0.07	2	234.972	16.82	
		−0.07 – −0.01	3	296.4371	21.22	
		−0.01 – 0.04	4	399.7398	28.62	
		0.04 – 0.20	5	343.8515	24.62	
7	**Flow Accumulation**	0.01 – 76114.36	1	1389.9605	99.52	**5.55**
		76114.36 – 271837.01	2	3.5576	0.25	

		271837.01 – 532800.54	3	1.3099	0.09	
		532800.54 – 869878.43	4	1.2427	0.09	
		869878.43 – 1386368.75	5	0.6374	0.05	
8	**Drainage Density (km/km²)**	0.01 – 1.48	1	369.9815	26.49	**4.66**
		1.48 – 2.68	2	403.1209	28.86	
		2.68 – 4.08	3	322.3119	23.08	
		4.08 – 5.83	4	226.8884	16.24	
		5.83 – 9.91	5	74.4322	5.33	
9	**Distance to Markets (m)**	5.41 – 3664.61	5	113.8416	8.15	**4.57**
		3664.61 – 6620.12	4	268.6629	19.24	
		6620.12 – 9364.52	3	368.4934	26.38	
		9364.52 – 12249.67	2	349.2513	25.01	
		12249.67 – 17949.58	1	296.4626	21.23	
10	**Distance to Water bodies**	0.01 – 211.86	5	51.2414	3.67	**3.01**
		211.86 – 498.50	4	136.5944	9.78	
		498.50 – 847.45	3	280.9135	20.11	
		847.45 – 1321.03	2	472.4173	33.82	
		1321.03 – 3177.95	1	454.5687	32.55	
11	**Distance to Hospitals (m)**	0.01 – 984.98	5	95.2297	6.82	**2.41**
		984.98 – 1742.65	4	212.6683	15.23	
		1742.65 – 2550.83	3	332.4738	23.80	
		2550.83 – 3535.81	2	431.1031	30.87	
		3535.81 – 6440.23	1	325.2604	23.29	
12	**Slope (°)**	0.01 – 1.42	5	15.3838	1.10	**2.21**
		1.42 – 2.43	4	114.7126	8.21	
		2.43 – 3.65	3	328.5984	23.53	
		3.65 – 5.78	2	561.2558	40.18	
		5.78 – 25.84	1	376.7552	26.97	

2.6 Microplastic susceptibility zonation

The reclassified factors and the AHP weights were combined by weighted linear combination in the raster calculator. For each cell, the microplastic susceptibility index (MPSI) was computed as the sum over the twelve criteria of the product of the criterion weight, expressed as a percentage, and the cell rating:

$$MPSI = \Sigma_i (W_i \times R_i)$$

where W_i is the AHP weight of criterion i in percent and R_i is its 1–5 rating at the cell. The continuous index ranged from 176.47 to 482.17 across the basin and was classified into five susceptibility classes,

namely Very Low, Low, Moderate, High and Very High, using the natural-breaks method. The unequal class widths that result from this classification reflect the natural grouping of index values rather than fixed intervals. The class boundaries and areal statistics are reported in Table 3, and the resulting zonation map is presented in Figure 14.

2.7 Village-level susceptibility analysis

To translate the continuous zonation into an administratively usable form, the susceptibility classes were extracted at the locations of 342 revenue villages within the basin. Each village was assigned a single dominant MPSZ class, and the reclassified 1–5 value of every factor was extracted at each village to build a village-by-factor matrix. This matrix supported two operations. First, class-wise factor profiles were computed as the mean rating of each factor within each MPSZ class, which describes how the factor composition changes across the susceptibility gradient. Second, the leading factors in each class were identified. Because a raw mean rating conflates the value of a factor with its importance in the model, the leading factors were determined from the weighted contribution, defined as the product of the mean rating and the AHP weight, rather than from the mean rating alone.

2.8 Statistical analysis

The susceptibility ratings are ordinal values on a 1–5 scale and are not normally distributed, so non-parametric methods were used throughout. Descriptive statistics summarised the central tendency and spread of each factor within each MPSZ class. Differences in factor ratings among the five classes were tested with the Kruskal–Wallis H test, which is the appropriate rank-based analogue of one-way analysis of variance for ordinal data across more than two groups. Because twelve factors were tested simultaneously, raw p-values were adjusted with the Benjamini–Hochberg false-discovery-rate procedure to control for multiple comparisons. The practical magnitude of each difference was quantified with the epsilon-squared effect size, which expresses the proportion of rank variance explained by class membership and is not inflated by the large sample size. Reporting the effect size alongside the significance test is essential, because with 342 villages a very small and practically unimportant difference can still be statistically significant. No additional statistical procedures were introduced.

3. Results and Discussion

3.1 Spatial characteristics of the susceptibility factors

The reclassified raster layers of parameters (Figs. 2–13) reveal a coherent spatial organization in which the strongest source and pathway signals cluster in the central and lower basin around the Cuddalore urban corridor and weaken toward the rural upland margins. Runoff was the most important factor that increases from the western uplands to the central plain. About two-fifths of the basin is in the two highest runoff categories (Fig. 2). This pattern links the monsoon rainfall to the flat surfaces where water flow gathers that makes runoff as the main factor in moving the soild waste to waterbodies (Ross et al., 2023). The anthropogenic source layers consistently reinforce the existing geographical patterns. Built-up land has been assigned as the highest Land Use and Land Cover (LULC) rating that covers approximately one-third of the basin which forming an almost continuous belt through the urban and peri-urban core (Fig. 3). Concurrently, the Normalized Difference Built-up Index (NDBI) characterizes this impervious footprint as a continuous surface (Fig. 7). Population density has been strongly concentrated with more than 70% of the basin in the lowest density class and the highest densities confined to compact urban cells (Fig. 4). The proximity layers to dump sites, industries and markets show the shortest distances, and therefore the highest ratings, in and around this same core (Figs. 5, 6 and 10), whereas hospital proximity is more evenly distributed (Fig. 11). The pathway-related terrain variables display the expected inverse texture. Slope is gentle across most of the basin, which favours retention (Fig. 13), and drainage density is moderate (Fig. 9). Flow accumulation is the clear outlier, because more than ninety-nine % of the basin falls in the single lowest class (Fig. 8). This near-uniformity is a genuine and expected property of a flow-accumulation surface, in which only the small fraction of cells that coincide with channels attains high values. The spatial alignment of concentrated sources with areas of high runoff and low slope in the central and lower basin represents the fundamental pattern that the composite index subsequently reflects.

3.2 AHP weights and criterion importance

The AHP assigned the largest weights to runoff (17.61 %), distance to dump sites (14.29 %), LULC (14.02 %) and population density (14.01 %), which together account for approximately 60% of the total weight (Table 2). Distance to industries (9.04 %) and NDBI (8.62 %) form an intermediate group, and the remaining six factors each contribute less than six %, with slope (2.21 %) the lowest. The consistency ratio of 0.052 indicates that this ordering reflects coherent judgement rather than arbitrary preference. The primary criteria collectively represent the two extremes of the source-to-pathway continuum: the runoff mechanism responsible for mobilizing particles and the concentrated anthropogenic sources that supply them. These criteria align with catchment studies that attribute riverine microplastic loading to the convergence of waste sources, population density, and runoff-driven transport (Ranjan et al., 2023; Hess et al., 2025). The higher weight given to runoff over the static source layers is appropriate for a

monsoon-driven basin in which delivery, rather than the mere presence of a source, governs whether particles reach the channel. The weighting must nonetheless be read with an awareness of conceptual overlap among the criteria, and the independence of the twelve layers should not be overstated. The hydrological group of runoff, flow accumulation, drainage density and slope shares a common dependence on terrain and drainage structure, so their information partly duplicates. Similarly, LULC, NDBI and population density all encode the intensity of urban development and are mutually correlated, because built-up land, impervious surface and dense population co-occur.

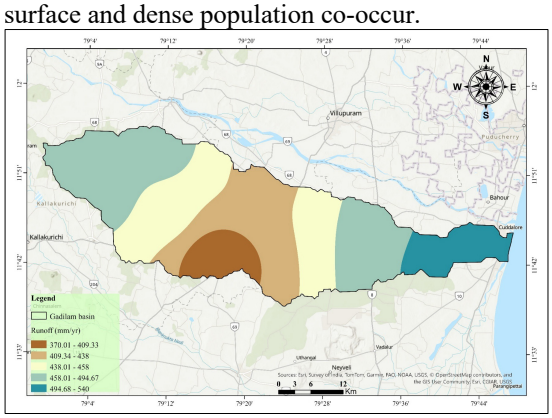


Figure 2: SCS – CN based Runoff estimation of the Gadilam river basin

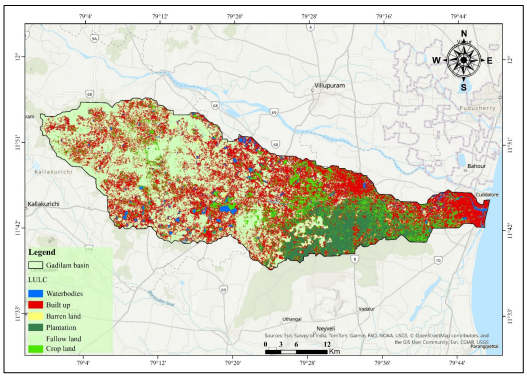


Figure 3: Land use and Landcover map of the Gadilam river basin

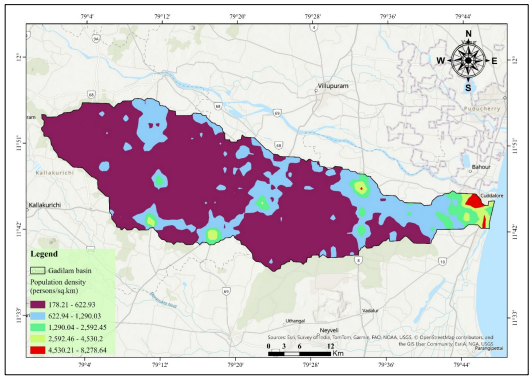


Figure 4: Population density of the Gadilam river basin

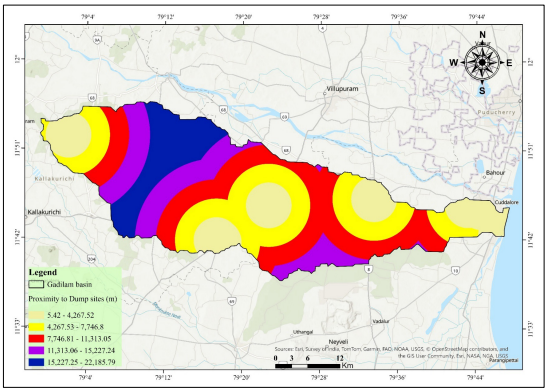


Figure 5: Proximity to Dump sites in the Gadilam river basin

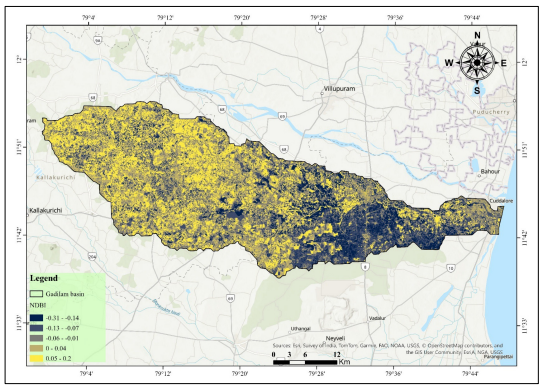


Figure 7: Estimation of NDBI from Landsat 9 satellite data of the Gadilam river basin

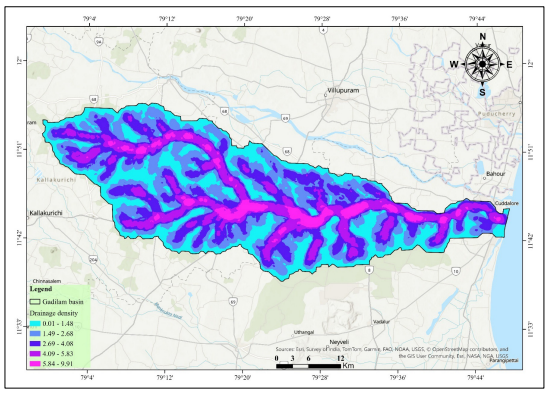


Figure 9: Extracted Drainage density from the SRTM (30m) DEM data of Gadilam river basin

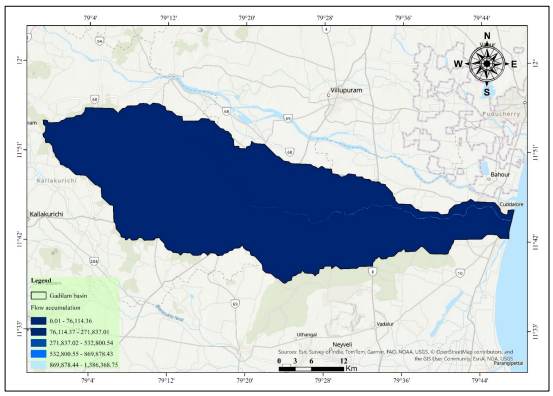


Figure 8: Extracted Flow accumulation from the SRTM (30m) DEM data of Gadilam river basin

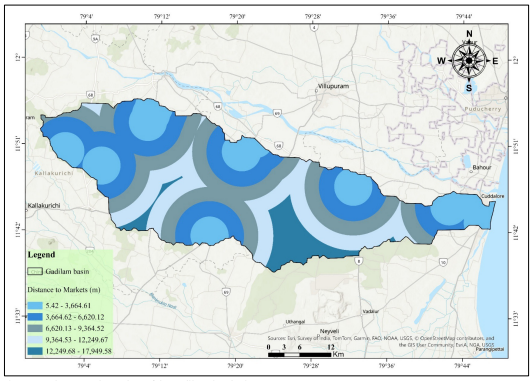


Figure 10: Distance to the markets of the Gadilam river basin

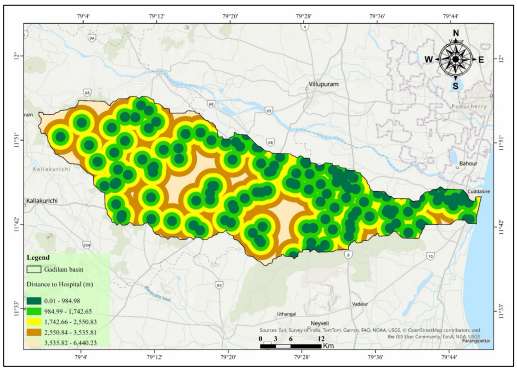


Figure 11: Disatnce to the Hospital in the Gadilam river basin

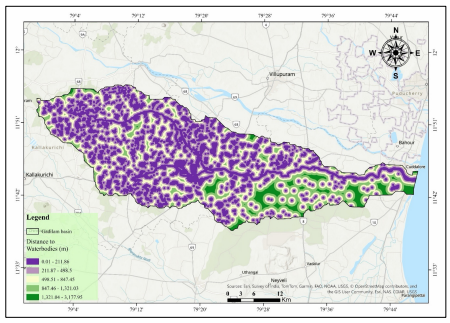


Figure 12: Distance to waterbodies in the Gadilam river basin

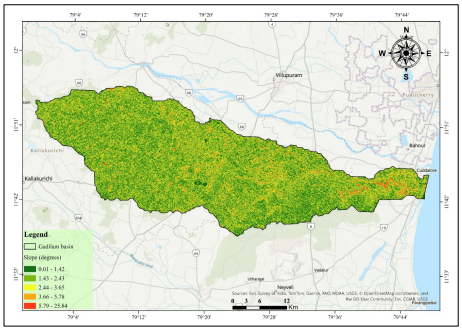


Figure 13: Extracted Slope map from the SRTM DEM of the Gadilam river basin

3.3 Microplastic susceptibility zonation

The weighted overlay produced a five-class susceptibility surface (Fig. 14; Table 3). Low susceptibility is the most extensive class at 35.60 % of the basin, followed by Moderate at 30.39 % and Very Low at 19.64 %, so that the lower three classes cover almost seventy % of the area. The High and Very High classes are spatially restricted and together occupy 14.38 %, comprising 8.84 and 5.54 % respectively.

Table 3. Areal distribution of the five microplastic susceptibility classes in the Gadilam River Basin.

Susceptibility class	Index range	Area (km²)	Area (%)
Very Low	176.47–257.99	274.36	19.64
Low	257.99–290.36	497.21	35.60
Moderate	290.36–328.72	424.42	30.39
High	328.72–380.27	123.41	8.84
Very High	380.27–482.17	77.40	5.54
Total		**1396.78**	**100.00**

The High and Very High zones are concentrated in the central and lower basin where concentrated waste sources, dense built-up land and elevated runoff coincide over gentle terrain. The mechanism is the alignment of a strong source term with an efficient delivery pathway in a low-gradient setting that favors retention (Gao et al., 2024; Xia et al., 2025). The resulted Microplastic Susceptibility zonation map shall be understood as a map of relative propensity, indicating where terrestrial microplastics are most likely to be generated and delivered not as measured concentration. (Beheshtimaal et al., 2024).

3.4 Village-level susceptibility distribution

The 342 villages located within the Gadilam river basin exhibit a distribution pattern akin to the areal configuration, albeit with a more pronounced central peak (Table 4). Moderate susceptibility contains the largest share at 33.63 % (115 villages), followed by Low at 30.41 % (104 villages) and Very Low at 22.22 % (76 villages). High and Very High susceptibility together account for 13.74 %, comprising 27 and 20 villages respectively. The close agreement between the village distribution and the areal distribution indicates that the zonation is stable when aggregated to administrative units and is not an artefact of a few large or small polygons. Although only forty-seven villages fall in the two highest classes, these are the units where source pressure and transport potential are jointly greatest, and they constitute a manageable and clearly bounded set for targeted intervention. The concentration of a larger group of 115 villages in the Moderate class is equally relevant, because these units sit close to the threshold at which additional urbanisation or waste-management failure could shift them upward. The village framing therefore converts a continuous surface into an actionable priority list, an approach that mirrors the use of spatial screening to direct limited monitoring resources in data-scarce basins (Ganie et al., 2024).

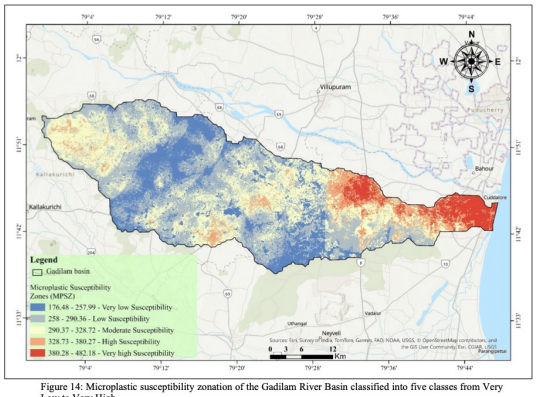


Figure 14: Microplastic susceptibility zonation of the Gadilam River Basin classified into five classes from Very Low to Very High.

3.5 Statistical analysis of the factors

The Kruskal–Wallis analysis (Table 5) shows that eleven of the twelve factors differ significantly among the susceptibility classes after false-discovery-rate correction, and only slope is non-significant. The factors separate into a clear hierarchy of practical importance. Distance to dump sites has the largest effect size ($\varepsilon^2 = 0.39$), followed by population density (0.36), runoff (0.26), LULC (0.26), distance to markets (0.21) and distance to industries (0.20). These six factors carry the differentiation between classes. A second group, comprising NDBI (0.09), distance to hospitals (0.09), drainage density (0.06) and distance to waterbodies (0.04), is statistically significant but explains little rank variance and therefore contributes marginally to discrimination. Flow accumulation (0.02) and slope (0.01) are effectively non-discriminating. The distributional form of the strongest factors across the five classes is illustrated by the violin plots in Figure 15.

Table 5. Kruskal–Wallis H, false-discovery-rate adjusted p-value, epsilon-squared effect size, and class mean ratings, ordered by effect size.

Factor	**H**	**adj. p**	**ε²**	**VL**	**L**	**Mod**	**Hi**	**VH**
Distance to dump sites	133.76	<0.001	0.39	2.18	2.64	3.71	4.26	4.90
Population density	124.42	<0.001	0.36	1.08	1.15	1.43	2.07	3.00
Runoff	92.69	<0.001	0.26	2.75	3.02	3.02	4.37	4.75
LULC	91.78	<0.001	0.26	2.54	3.51	3.91	3.74	5.00
Distance to markets	75.01	<0.001	0.21	2.54	3.28	3.40	4.26	4.90
Distance to industries	70.35	<0.001	0.20	3.49	2.91	3.39	4.59	4.80
NDBI	35.23	<0.001	0.09	2.66	3.66	3.42	3.07	3.75
Distance to hospitals	33.16	<0.001	0.09	3.33	3.16	3.71	4.22	4.50
Drainage density	23.71	<0.001	0.06	1.97	2.29	2.68	2.44	2.75
Distance to waterbodies	19.11	<0.001	0.04	3.82	4.15	4.17	3.56	3.60
Flow accumulation	11.67	0.022	0.02	1.00	1.00	1.00	1.11	1.00
Slope	6.13	0.190	0.01	3.78	4.00	3.92	3.67	3.45

The discriminating factors are the same variables that received the highest AHP weights, which provides independent, data-driven support for the expert weighting. Distance to dump sites is both the most heavily weighted proximity criterion and the strongest statistical separator, and its mean rating

rises monotonically from 2.18 in Very Low to 4.90 in Very High (Table 5). This convergence between a knowledge-based weight and an empirical effect size is a useful internal validation, because the two were derived independently. It also localises the dominant source signal to informal waste disposal, in agreement with evidence that open dump sites are concentrated terrestrial microplastic sources whose influence declines with distance (Hess et al., 2025; Chamanee et al., 2024). The weak performance of flow accumulation is a direct consequence of its near-uniform classification rather than a statement about the irrelevance of hydrological convergence,

3.6 Dominant factors across the susceptibility gradient

The systematic variation in factor profiles from Very Low to Very High susceptibility is significant, and the method of summarizing this change is crucial. In this dataset, a naive mean-rating ranking would prioritize distance to waterbodies and slope as the leading factors in the lower classes. However, these two variables possess the lowest AHP weights and the smallest effect sizes, with distance to waterbodies actually decreasing toward the higher classes. Their high average ratings are an artefact of the rating scale rather than an indicator of susceptibility. The weighted contribution, defined as the product of a factor's class mean rating and its AHP weight corrects this distortion and identifies the factors that genuinely contribute to the composite index in each class (Table 4). Based on this analysis, runoff, LULC, and distance to dump sites dominate the higher classes. Runoff increases from a weighted contribution of approximately 0.48 in Very Low to 0.84 in Very High, LULC from 0.36 to 0.70, and distance to dump sites from a subordinate position in the lowest class to 0.70 in Very High. This trajectory aligns with the effect sizes in Table 5 and the underlying process model. As susceptibility increases, villages move closer to waste sources, occupy more built-up land, and experience higher runoff, resulting in a concurrent rise in source strength and delivery potential. This mechanism, wherein urbanization and waste pressure elevate the terrestrial load while runoff governs its mobilization, is consistently reported for urban and peri-urban river reaches (Ranjan et al., 2023; Gao et al., 2024). The present analysis demonstrates the same coupling expressed across an ordered susceptibility gradient.

Table 4. Village distribution and leading weighted-contribution factors across MPSZ classes. Weighted contribution is the product of the class mean rating and the AHP weight (fraction).

MPSZ class	Villages	%	Leading factors by weighted contribution
Very Low	76	22.22	Runoff (0.48); LULC (0.36); Distance to industries (0.32)
Low	104	30.41	Runoff (0.53); LULC (0.49); Distance to dump sites (0.38)
Moderate	115	33.63	LULC (0.55); Runoff (0.53); Distance to dump sites (0.53)
High	27	7.89	Runoff (0.77); Distance to dump sites (0.61); LULC (0.52)
Very High	20	5.85	Runoff (0.84); LULC (0.70); Distance to dump sites (0.70)

3.7 Correlation structure among factors and susceptibility classes

The correlation heat map (Fig. 16) provides a compact synthesis of the associations between the twelve factor ratings and the susceptibility classification across the 342 villages, and its structure corroborates the hierarchy established by the AHP weights and the Kruskal–Wallis effect sizes. The susceptibility class is most strongly and positively associated with distance to dump sites, population density, runoff, LULC, distance to markets and distance to industries, the same six factors that carry the largest effect sizes in Table 5 and whose class mean ratings rise monotonically or near-monotonically from Very Low to Very High. This convergence suggests that the composite index is driven principally by the joint intensification of waste-source proximity, human occupancy and runoff generation, and it is consistent with the

weight structure. A second group of factors, comprising NDBI, distance to hospitals and drainage density, shows weaker positive associations with the susceptibility class, in agreement with their modest effect sizes. Distance to waterbodies and slope display weak negative associations, reflecting the decline of their mean ratings toward the higher classes (from 3.82 to 3.60 and from 3.78 to 3.45 respectively), and flow accumulation is essentially unassociated with class membership because almost all villages share the same lowest rating. These weak or inverse associations confirm that the low-weight factors neither drive nor distort the zonation.

The heat map also exposes the internal correlation structure among the factors themselves. The anthropogenic variables, comprising LULC, NDBI, population density and the proximity measures to dump sites, industries, markets and hospitals, form a mutually and positively associated cluster, which is expected because built-up land, impervious surface, dense population and waste or service infrastructure co-occur within the urban core. The hydrological and terrain variables, comprising runoff, drainage density, flow accumulation and slope, share a common dependence on terrain and drainage structure and show associations among themselves that are largely separate from the anthropogenic block. The block structure demonstrates redundancy within each group, suggesting that the urban-development signal is incorporated into the composite through several partially overlapping layers. The patterns are characterized exclusively in associational terms; the heat map summarizes co-variation across villages without establishing causal relationships among the factors or between any factor and the observed microplastic occurrence.

3.8 Source–pathway interpretation

Synthesizing spatial, weighting, and statistical evidence provides a coherent source-to-pathway account of susceptibility within the basin. The source term is determined by concentrated anthropogenic activities. Informal dump sites, dense populations, developed land, market clusters, and industrial establishments converge in the central and lower basin, with their combined influence captured by the four highest-weighted and most impactful factors. The prominence of dump-site proximity is significant, as open dumping and burning of solid waste are increasingly recognized as terrestrial microplastic sources, with soil concentrations potentially matching or exceeding those from other diffuse pathways (Hess et al., 2025; Kabir et al., 2023). Additionally, industrial and market clusters contribute fiber and packaging inputs typical of urban catchments in developing countries (Magalhães et al., 2024). The pathway term is governed by runoff, drainage, and terrain. Runoff serves as the mechanism connecting these sources to the channel, with its high weight and effect size placing it at the core of the transport process. Surface runoff over impervious and disturbed surfaces is a well-documented non-point pathway that delivers particles to receiving waters in pulses during rainfall (Ross et al., 2023; Cho et al., 2023), and the monsoon concentration of rainfall in this basin amplifies that delivery. Drainage density and slope modulate the pathway by controlling connectivity and residence time, with gentle gradients favoring low-energy settings where particles settle and are retained. The receiving and retention term is represented by the river network, connected water bodies, and low-gradient zones. However, the strength of the source-to-pathway relationship is not uniform and depends on hydrological connectivity, which explains part of the spatial heterogeneity of the susceptibility surface (Fig. 14). Where sources are close to well-connected channels, delivery is efficient and susceptibility is high, whereas equally intense sources on poorly connected or steeper ground contribute less to the channel. This connectivity dependence aligns with observations that riverine microplastic transport and retention vary significantly with the connectivity context of the reach (Xia et al., 2025), cautioning against interpreting the source layers in isolation from the pathway layers.

3.8 Management priorities

Because the dominant factors are anthropogenic and spatially concentrated, the findings support targeted rather than generic intervention. The primacy of dump-site proximity indicates that securing, relocating or remediating informal disposal sites in the central and lower basin would remove the single strongest source signal, and the same locations should be prioritized for the interception of leachate and wind-blown debris (Chamanee et al., 2024). The high weights of runoff and NDBI point to urban runoff management on impervious surfaces, where source-control measures and drainage interception such as retention structures and sustainable drainage can reduce the wash-off that mobilizes particles during the monsoon (Ross et al., 2023). Industrial and market clusters identified by the proximity layers warrant source-specific controls, including effluent screening at textile and manufacturing units and improved solid-waste handling in market areas (Magalhães et al., 2024). Drainage interception should be concentrated where high runoff and dense channels coincide, so that limited engineering effort is placed on the reaches that deliver the most. Finally, the twenty Very High and twenty-seven High susceptibility villages define a bounded monitoring network. Directing the first field sampling campaigns to these forty-seven units would test the model against measured concentrations while using scarce monitoring capacity efficiently, an approach well suited to data-

poor basins where comprehensive sampling is impractical (Ganie et al., 2024).

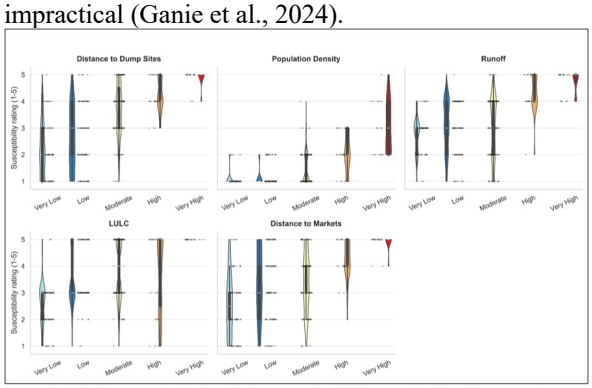
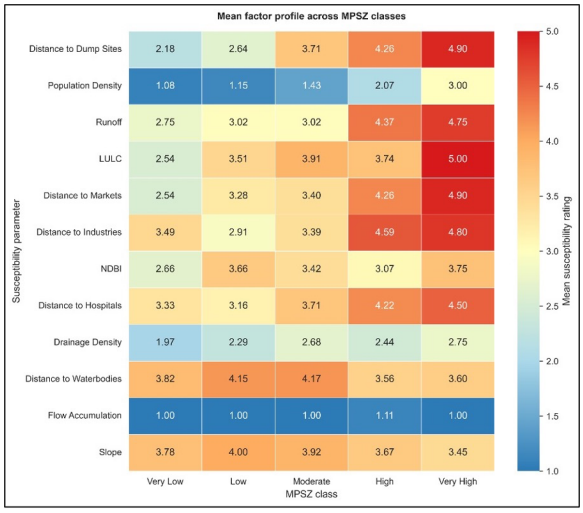


Figure 15: Violin plot represents distribution of the strongest susceptibility factors across MPSZ zonation across the classes



Conclusion

This study developed the first basin-scale microplastic susceptibility zonation for the Gadilam River Basin, Tamil Nadu, by integrating twelve source, pathway and terrain criteria within a GIS-based analytic hierarchy process. The pairwise comparison yielded an internally consistent weighting scheme (consistency ratio 0.052) in which runoff (17.61%), distance to dump sites (14.29%), land use/land cover (14.02%) and population density (14.01%) together accounted for approximately sixty % of the total weight, reflecting the joint control of anthropogenic source pressure and monsoon-driven transport on relative susceptibility. The weighted overlay classified the basin into five susceptibility zones. The Very Low, Low and Moderate classes together cover almost seventy % of the area, while the High (8.84%, 123.41 km²) and Very High (5.54%, 77.40 km²) classes are spatially restricted and concentrate in the central and lower basin, where informal dump sites, dense built-up land, market and industrial clusters and elevated runoff coincide over gentle terrain. Aggregation to administrative units produced a closely matching distribution across the 342 revenue villages, with 27 villages in the High class and 20 in the Very High class, indicating that the zonation is stable when translated into an administratively actionable form.Non-parametric analysis provided independent, data-driven support for the expert weighting. Eleven of the twelve factors differed significantly among the susceptibility classes after false-discovery-rate correction, and the largest epsilon-squared effect sizes belonged to distance to dump sites (0.39), population density (0.36), runoff (0.26) and LULC (0.26), the same factors that received the highest AHP weights. Weighted-contribution analysis confirmed that runoff, LULC and dump-site proximity genuinely build the composite index in the higher classes, whereas high mean ratings for low-weight factors such as slope and distance to waterbodies are artefacts of the rating scale rather than signals of susceptibility. The correlation structure among the factors further showed that the anthropogenic variables form a mutually associated cluster and the hydrological variables another, indicating partial redundancy that reinforces the interpretation of the index as relative rather than additive. The findings support targeted rather than generic intervention. Securing, relocating or remediating informal dump sites in the central and lower basin would address the single strongest source signal; urban runoff management on impervious surfaces would reduce the monsoon wash-off that mobilises particles; and source-specific controls at industrial and market clusters would limit fibre and packaging inputs. The forty-seven High and Very High susceptibility villages define a bounded network for the first field sampling campaigns, allowing scarce monitoring capacity to be deployed where source pressure and transport potential are jointly greatest. The principal limitations are the subjective character of the elicited AHP weights, the partial redundancy among correlated criteria, the use of proxy indicators such as Euclidean distance and population density, the sensitivity of the result to the 30 m resolution and natural-breaks thresholds, the weak discriminatory power of flow accumulation at village centroids, and, above all, the absence of field microplastic concentration data. The susceptibility map therefore indicates where terrestrial microplastics are most likely to be generated and delivered, not where contamination has been measured. External validation against measured concentrations in the High and Very High villages, together with a formal sensitivity analysis of the weights and improved representations of flow accumulation and drainage-controlled transport paths, constitutes the essential next step before the zonation is applied to regulatory decisions. Subject to that validation, the framework offers a transferable, data-efficient screening tool for prioritising microplastic monitoring and mitigation in data-scarce river basins.

References:

Acciavatti, A., Arora, S., Warner, M., Chamberlain, A., Smoot, J.C., Deep, N.R., Hanly, C.G., 2024. Remote sensing for sustainable river management: Estimating riverscape vulnerability for Ganga, the world's most densely populated river basin. arXiv preprint arXiv:2412.12113. https://doi.org/10.48550/arXiv.2412.12113 [Preprint; also posted on EarthArXiv. If a peer-reviewed version has since appeared, cite that version instead.]

Beheshtimaal, A., Alamdari, N., Wang, B., Kamali, M., Salehi, M., 2024. Understanding the dynamics of microplastics transport in urban stormwater runoff: Implications for pollution control and management. Environmental Pollution 356, 124302. https://doi.org/10.1016/j.envpol.2024.124302

Chamanee, G., Sewwandi, M., Wijesekara, H., Vithanage, M., 2024. Occurrence and abundance of microplastics and plasticizers in landfill leachate from open dumpsites in Sri Lanka. Environmental Pollution 350, 123944. https://doi.org/10.1016/j.envpol.2024.123944

Cho, Y., Shim, W.J., Ha, S.Y., Han, G.M., Jang, M., Hong, S.H., 2023. Microplastic emission characteristics of stormwater runoff in an urban area: Intra-event variability and influencing factors. Science of the Total Environment 866, 161318. https://doi.org/10.1016/j.scitotenv.2022.161318

Gao, [initials], 2024. A review on microplastics in major European rivers. WIREs Water 11, e1713. https://doi.org/10.1002/wat2.1713 [Complete the author list from the DOI; confirm this is the intended Gao et al. (2024) — see Section 2 note.]

Han, N., Zhao, Q., Ao, H., Hu, H., Wu, C., 2022. Horizontal transport of macro- and microplastics on soil surface by rainfall induced surface runoff as affected by vegetations. Science of the Total Environment 831, 154989. https://doi.org/10.1016/j.scitotenv.2022.154989

Hess, K.Z., Forsythe, K.R., Wang, X., Arredondo-Navarro, A., Tipling, G., Jones, J., Mata, M., Hughes, V., Martin, C., Doyle, J., Scott, J., Minghetti, M., Jilling, A., Cerrato, J.M., El Hayek, E., Gonzalez-Estrella, J., 2025. Emerging investigator series: Open dumping and burning: an overlooked source of terrestrial microplastics in underserved communities. Environmental Science: Processes & Impacts 27, 52–62. https://doi.org/10.1039/D4EM00439F

Jambeck, J.R., Geyer, R., Wilcox, C., Siegler, T.R., Perryman, M., Andrady, A., Narayan, R., Law, K.L., 2015. Plastic waste inputs from land into the ocean. Science 347, 768–771. https://doi.org/10.1126/science.1260352

Kabir, M.S., Wang, H., Luster-Teasley, S., Zhang, L., Zhao, R., 2023. Microplastics in landfill leachate: Sources, detection, occurrence, and removal. Environmental Science and Ecotechnology 16, 100256. https://doi.org/10.1016/j.ese.2023.100256

Kamani, H., Ghayebzadeh, M., Azari, A., Ganji, F., 2024. Characteristics of microplastics in a hospital wastewater treatment plant effluent and hazard risk assessment. Environmental Processes 11, 15. https://doi.org/10.1007/s40710-024-00694-7

Kay, P., Hiscoe, R., Moberley, I., Bajic, L., McKenna, N., 2018. Wastewater treatment plants as a source of microplastics in river catchments. Environmental Science and Pollution Research 25, 20264–20267. https://doi.org/10.1007/s11356-018-2070-7

Lebreton, L.C.M., van der Zwet, J., Damsteeg, J.-W., Slat, B., Andrady, A., Reisser, J., 2017. River plastic emissions to the world's oceans. Nature Communications 8, 15611. https://doi.org/10.1038/ncomms15611

Lodh, A., Shafi, M., Goel, S., 2025. Microplastics in municipal solid waste landfill leachate and their removal in treatment units: A perspective of controlled and uncontrolled landfills. Environmental Pollution 369, 125853. https://doi.org/10.1016/j.envpol.2025.125853

Magalhães, S., [co-authors], 2024. Insights on microplastic contamination from municipal and textile industry effluents and their removal using a cellulose-based approach. Polymers 16, 2803. https://doi.org/10.3390/polym16192803 [Complete the author list from the DOI.]

Manikanda Bharath, K., Natesan, U., Vaikunth, R., Praveen Kumar, R., Ruthra, R., Srinivasalu, S., 2021. Spatial distribution of microplastic concentration around landfill sites and its potential risk on groundwater. Chemosphere 277, 130263. https://doi.org/10.1016/j.chemosphere.2021.130263

McNulty, K., Nahar, K., 2024. Geospatial modelling predicts agricultural microplastic hotspots from biosolid application risks. Agronomy 15, 47. https://doi.org/10.3390/agronomy15010047 [Published online 27 December 2024; issue dated 2025. See Section 3 regarding attribution.]

Mitrano, D.M., Wick, P., Nowack, B., 2021. Placing nanoplastics in the context of global plastic pollution. Nature Nanotechnology 16, 491–500. https://doi.org/10.1038/s41565-021-00888-2

Prasanna, M.V., Chidambaram, S., Srinivasamoorthy, K., 2010. Statistical analysis of the hydrogeochemical evolution of groundwater in hard and sedimentary aquifers system of Gadilam river basin, South India. Journal of King Saud University – Science 22, 133–145. https://doi.org/10.1016/j.jksus.2010.04.001 [Confirm page range against the publisher record.]

Range, D., Scherer, C., Stock, F., Ternes, T.A., Hoffmann, T.O., 2023. Hydro-geomorphic perspectives on microplastic distribution in freshwater river systems: A critical review. Water

Research 245, 120567. https://doi.org/10.1016/j.watres.2023.120567
Ranjan, K., Khudsar, F.A., Kumar, R., 2023. Urbanization and population resources affect microplastic concentration in the surface water of the river Ganga. Journal of Hazardous Materials Advances 11, 100342. https://doi.org/10.1016/j.hazadv.2023.100342
Ross, M.S., Loutan, A., Groeneveld, T., Molenaar, D., Kroetch, K., Bujaczek, T., Kolter, S., Moon, S., Huynh, A., Khayam, R., Franczak, B.C., Camm, E., Arnold, V.I., Ruecker, N.J., 2023. Estimated discharge of microplastics via urban stormwater during individual rain events. Frontiers in Environmental Science 11, 1090267. https://doi.org/10.3389/fenvs.2023.1090267
Saaty, T.L., 1980. The Analytic Hierarchy Process: Planning, Priority Setting, Resource Allocation. McGraw-Hill, New York.
Saaty, T.L., 2008. Decision making with the analytic hierarchy process. International Journal of Services Sciences 1, 83–98. https://doi.org/10.1504/IJSSCI.2008.017590
Ta, A.T., Babel, S., 2023. Occurrence and spatial distribution of microplastic contaminated with heavy metals in a tropical river: Effect of land use and population density. Marine Pollution Bulletin 191, 114919. https://doi.org/10.1016/j.marpolbul.2023.114919
Talbot, R., Chang, H., 2022. Microplastics in freshwater: A global review of factors affecting spatial and temporal variations. Environmental Pollution 292, 118393. https://doi.org/10.1016/j.envpol.2021.118393
Thompson, R.C., Olsen, Y., Mitchell, R.P., Davis, A., Rowland, S.J., John, A.W.G., McGonigle, D., Russell, A.E., 2004. Lost at sea: Where is all the plastic? Science 304, 838. https://doi.org/10.1126/science.1094559
Xia, F., Yang, W., Zhao, H., Cai, Y., Tan, Q., 2025. Occurrence characteristics and transport processes of riverine microplastics in different connectivity contexts. npj Clean Water 8, 1. https://doi.org/10.1038/s41545-024-00424-4
Yu, F., Yu, W., Zhao, Y., Liang, Y., Hu, J., Liu, R., Chen, S., Chen, Q., Liu, Y., Zheng, X., Li, X., 2025. Correcting microplastic pollution and risk assessment in Chinese watersheds. Environmental Pollution. [Verified title, authors and journal; complete the volume, article number and DOI from the publisher record before submission.]
Zha, Y., Gao, J., Ni, S., 2003. Use of normalized difference built-up index in automatically mapping urban areas from TM imagery. International Journal of Remote Sensing 24, 583–594. https://doi.org/10.1080/01431160304987